



# HHS Public Access

Author manuscript

*Birth Defects Res.* Author manuscript; available in PMC 2020 August 15.

Published in final edited form as:

*Birth Defects Res.* 2019 August 15; 111(14): 999–1012. doi:10.1002/bdr2.1398.

## Embryonic cell migratory capacity is impaired upon exposure to glucose *in vivo* and *in vitro*

Nils J. Herion<sup>1,2</sup>, Claudia Kruger<sup>2</sup>, Jaroslaw Staszkiwicz<sup>2</sup>, Claudia Kappen<sup>2</sup>, J. Michael Salbaum<sup>3</sup>

<sup>1</sup>University of Heidelberg Medical School, Heidelberg, Germany

<sup>2</sup>Departments of Developmental Biology, Pennington Biomedical Research Center, 6400 Perkins Road, Baton Rouge, LA 70808, USA

<sup>3</sup>Departments of Regulation of Gene Expression, Pennington Biomedical Research Center, 6400 Perkins Road, Baton Rouge, LA 70808, USA

### Abstract

**Background:** Impairments in cell migration during vertebrate gastrulation lead to structural birth defects, such as heart defects and neural tube defects. These defects are more frequent in progeny from diabetic pregnancies, and we have recently provided evidence that maternal diabetes leads to impaired migration of embryonic mesodermal cells in a mouse model of diabetic pregnancy.

**Methods:** We here report the isolation of primary cell lines from normal and diabetes-exposed embryos of the non-obese diabetic (NOD) mouse strain, and characterization of their energy metabolism and expression of nutrient transporter genes by quantitative Real-Time PCR.

**Results:** Expression levels of several genes in the glucose transporter and fatty acid transporter gene families were altered in diabetes-exposed cells. Notably, primary cells from embryos with prior *in vivo* exposure to maternal diabetes exhibited reduced capacity for cell migration *in vitro*.

**Conclusions:** Primary cells isolated from diabetes-exposed embryos retained a “memory” of their *in vivo* exposure, manifesting in cell migration impairment. Thus, we have successfully established an *in vitro* experimental model for the mesoderm migration defects observed in diabetes-exposed mouse embryos.

### Introduction

Neural tube defects occur with higher incidence in human pregnancies affected by maternal diabetes during the first trimester (Kucera 1971, Mills, Baker et al. 1979, Martinez-Frias 1994). Although hyperglycemia in the mother is believed to create the conditions that impair neural tube closure (Kousseff 1999, Ornoy, Reece et al. 2015), the causative mechanisms for specific birth defects in human diabetic pregnancies are unknown.

The laboratory mouse has become a popular experimental model for neural tube defects, due to the practical advantages of short gestation span and the availability of large collection of

mutants that enable investigations into the role of specific molecules and pathways in defective neural tube closure (Juriloff and Harris 2000, Harris and Juriloff 2010). By now, more than 400 genes that are required for neural tube closure are known, by virtue of offspring with homozygous gene disruptions presenting with neural tube defects, and 34.5% of these genes exhibit altered expression in embryos from mouse diabetic pregnancies (Salbaum and Kappen 2010). Yet, how the products encoded by these genes control the morphogenetic events of neural tube closure, i.e. movement of tissues and cells in the developing embryo, particularly in conditions of diabetic pregnancy, is less well understood.

We have recently shown, using the NOD (non-obese diabetic) mouse strain that has a high rate of neural tube defects (Otani, Tanaka et al. 1991), that maternal diabetes is associated with impaired cell migration during gastrulation, the process in which mesoderm is generated (Salbaum, Kruger et al. 2015). Explants of primitive streak tissue from gastrulation stage embryos exhibited less outgrowth in culture when the embryo was derived from a diabetic as compared to a normal pregnancy. We identified the affected cells as of mesodermal origin, indicating that cell specification was not altered. We therefore concluded that maternal diabetes specifically affects cell migration of mesodermal cells.

In this study, we sought to establish a tissue culture model of mesodermal cell migration that would enable detailed investigations of the cellular and molecular mechanisms underlying the pathogenesis of neural tube defects in diabetic pregnancies. We therefore established primary cell lines from embryos of normal and diabetic mouse females, and assessed the capacity of these cells to migrate under conditions of exposure to high and low concentrations of glucose. The combined evidence from several independent primary cell lines indicates that cell migration is impaired by exposure to high glucose conditions *in vitro* and *in vivo*.

## Materials and Methods

### Isolation of primary embryonic cells from a mouse diabetic pregnancy model

As a mouse model for diabetic pregnancy we used the NOD (non-obese-diabetic) mouse strain (Jackson Laboratories stock # 001976)(Otani, Tanaka et al. 1991). Females of this strain become diabetic spontaneously around 12–17 weeks. Blood glucose levels were measured weekly by glucometer, and mice were considered diabetic when the reading exceeded 250 mg/dl (13.875 mmol/l). For comparison, blood glucose levels in non-diabetic dams were 117.3 mg/dl  $\pm$  21.5 (n=10). Diabetic females and non-diabetic females of the same age cohort were then mated to non-diabetic NOD males (Salbaum, Kruger et al. 2015). Blood glucose levels were measured again before euthanasia. Primary mouse embryonic cells were prepared as described by Robertson (Robertson 1987) for preparation of feeder layer cells. Embryos were isolated from pregnant females at E12.5 (with the morning of detection of a copulation plug counted as E0.5). Only embryos were used that were of the same developmental stage when compared between normal and diabetic pregnancies. Cells were plated on 0.1% gelatin-coated plastic tissue culture plates in either low or high glucose-containing DMEM medium supplemented with Glutamax, non-essential amino-acids, 100 units of Penicillin/Streptomycin, 0.1%  $\beta$ -mercaptoethanol and 16% fetal calf serum (Hyclone). Primary cells from embryos of normal pregnancies were grown in low glucose

concentration, reflecting normoglycemic conditions *in vivo*, and cells from diabetic pregnancies were initially cultured in high glucose concentration mimicking the hyperglycemic conditions *in vivo*. Cells were expanded to Passage 6, after which each line was split into both high and low glucose-containing maintenance media, and adapted to the media for 3 more passages. At Passage 9, multiple aliquots were frozen for future experimental use.

For experimental use, cell aliquots were thawed and plated in 0.1% gelatin-coated T75 tissue culture flasks, where all cell lines were maintained in two conditions in parallel in media with high and low glucose concentration, respectively. After confluence was reached for the first time (typically after three to four days), cells were passaged every three days by splitting the contents from one flask into three new flasks of the same size. Passaging was performed by incubating cells with 0.25% Trypsin 0.04% EDTA (Sigma) for 5 minutes, after which the digestion was stopped by adding serum-containing medium. Once the desired cell quantities were reached, cells were trypsinized off for use in the respective assay. As much as possible, cells used in a given assay were of comparable passage, and assay results were only combined from cells within a range of two passages.

## Medium

The culture media for maintenance after passage 6 were based on DMEM supplemented with Glutamax, non-essential amino-acids, 100 units of Penicillin/Streptomycin and 0.1%  $\beta$ -mercaptoethanol. Low glucose medium contained 1 g/l D-glucose (5.55 mmol/l), high glucose medium contained 4.5g/l D-glucose (24.97 mmol/l), and both media had a concentration of 110 mg/l Sodium Pyruvate and 10% Fetal Bovine Serum (Hyclone). All other media ingredients came from GIBCO.

## Migration Assays

Cells were plated in 24-well plates and allowed to adhere and grow for 24 hours to reach confluency. Cells were scratched from one half of each well after a broad longitudinal scratch through the middle of the well. Supernatant was removed and fresh medium containing high or low concentrations of glucose was added for the respective assay condition, and plates were placed in a humidified 37° chamber with 5% CO<sub>2</sub> atmosphere. Plates were then videographed over 26 hours on a Leica TIRF microscope with time-lapse images taken every 10 minutes, producing 157 frames, including the first frame at time = 0 minutes. Analysis of cell migration was performed for all conditions at frame 145, corresponding to 24 hours after the scratch was made. A vertical line was drawn (Leica Application Suite) at the edge of the scratch in frame 1 (= 0 minutes) to mark the starting position, from which net migration distance was measured for individual cells as the length of a straight distance perpendicular to the start line (frame 1) to the individual cell location in frame 145, respectively. As many video recordings as possible were made along each scratch and videos of non-overlapping fields of view analyzed for each well. Each assay condition was represented by multiple wells as noted in the Figure legends. Multiple cell travel distance measurements were averaged by well (see Figure legends), and then averages were calculated for all wells with the same assay condition. Cell lines were assayed under two conditions of glucose concentration in the medium, i.e. low and high, respectively.

### Computer-assisted cell counting

Freshly thawed cells were seeded at 30,000 cells/well into gelatin-coated 24-well plates in respective media conditions, with three plates in identical layout: 6 time points and 4 cell lines. At given time points, media were aspirated from one well each per plate and cell line, and cells stained with Hoechst 33342 (1:10,000) on the plate. Using a preheated cell incubation chamber, 5 images/well were taken on the Leica TIRF microscope in identical sequence for each well. After all 20 pictures were taken for the 4 stained wells of a plate, the 24-well plate was returned to normal incubation until the next time point. The process of photography took less than 10 minutes per time point and plate.

Image analysis was performed in ImageJ as follows: After background subtraction and color adjustment to eliminate minor signals from dirt or serum particles, each image was processed in “Binary->Covert to Mask” and “Binary->Watershed” to set thresholds so that two adjacent cells are detected as two distinct entities, followed by “Analyze->Analyze Particles” with the assumption that number of particles are proportional to cell number.

For each well, the particle numbers from 5 images were added, and then averaged between the three wells containing the same cell line. The first time point was normalized to 100%, and counts at subsequent time points were expressed as percentages of the first time point.

### Measurements of cellular energy metabolism

The Seahorse XF24 Extracellular Flux Analyzer (Seahorse Bioscience) was used to measure the Oxygen Consumption Rate (OCR) and Extracellular Acidification Rate (ECAR) according to the manufacturer’s recommendation. Briefly, XF-24 cell culture plates (Seahorse) were coated with 0.1% gelatin followed by a cell inoculation. Mouse primary embryonic fibroblasts (passage 8–9) were plated at density of  $3 \times 10^4$  cells per well and incubated overnight at 37°C in 5% CO<sub>2</sub> in a humidified incubator. Prior to the assay, growth medium was replaced with assay medium (Seahorse XF Base Medium, 0.025 M glucose, pH 7.4), and the cells were incubated at 37°C in a CO<sub>2</sub>-free incubator for 30 min. Following baseline measurements, the assay wells were sequentially injected with oligomycin (ATP synthase inhibitor; 2 μM final concentration), carbonyl cyanide 4-(trifluoromethoxy) phenylhydrazone (FCCP; mitochondrial respiration uncoupler; 2 μM final concentration), antimycin (mitochondrial electron transport blocker; 4 μM final concentration), and glucose (200 mM final concentration). Two measurements of OCR and ECAR for each compound were obtained, and the values were normalized to a pre-exposure baseline. Data are expressed as a percentage of OCR or ECAR change over baseline.

### Gene expression analyses

Total RNA from cells was isolated using TRIzol Reagent (Thermo Fisher Scientific). RNA cleanup and on-column DNase I digestion was performed using the RNeasy Mini Kit from Qiagen. RNA quantity was determined with the NanoDrop ND-1000 Spectrophotometer (Thermo Fisher Scientific). Quality of RNA was assessed using the RNA 6000 Nano chip designed for the Agilent 2100 Bioanalyzer instrument (Agilent Technologies). The RNA Integrity Number (RIN) obtained was above 9 for all samples. For each sample, 1 μg of RNA

was subjected for reverse transcription reaction (High-Capacity cDNA Reverse Transcription Kit, Applied Biosystems).

Expression levels of nutrient transporters were measured by quantitative RT-PCR. Primer pairs were designed using Primer Express Software v3.0 (Applied Biosystems) and synthesized by Integrated DNA Technologies (Coralville, IA). Where possible, primer pairs were designed to span an exon-exon boundary (Table 1) to exclude potential contamination with genomic DNA from detection in the assay. PCR reactions were run with the equivalent of 2ng cDNA (estimated to be equivalent to the amount of RNA input into the reverse transcription reaction) in 10µl volume per sample using iTaq Universal SYBR Green Supermix (Bio Rad) on the 7900HT Sequence Detection System (Applied Biosystems) with default settings, dissociation curves included. The Comparative C<sub>T</sub> Method was used for quantification of gene expression (User Bulletin #2, Applied Biosystems). For each primer pair, the actual amplification efficiency was calculated (Table 1) and implemented in the formula to calculate fold-changes as described before (Kruger and Kappen 2010). The geometric means of measurements for Polymerase epsilon 4 (Pole4) and PAK interacting protein 1 (Pak1) gene expression were used as the references for normalization of nutrient transporter expression to derive Ct values. For each sample, triplicate aliquots were measured for technical replication, and these triplicate values were used to evaluate statistical significance.

### Statistical analysis

Statistical analysis of comparisons between conditions was conducted using T-tests, assuming unequal variances and two-sided p-values. ANOVA with Bonferroni post-hoc correction was used to adjust for multiple comparisons. P-values smaller than p=0.05 were considered significant. One-way ANOVA was used to perform statistical analysis of Seahorse measurements as implemented in the analysis software package supplied by the manufacturer. Two-factor ANOVA was applied to comparisons across the independent variables “exposure” and “glucose concentration”, and to identify potential interactions between these variables.

### Results

Primary cells were isolated from mouse embryos from pregnant dams of the non-obese diabetic strain (NOD) that had either normal or diabetic (>250 mg/dl) blood glucose levels. For the first 6 passages, cells were grown according to their origin in media containing either low or high glucose concentrations, to mimic normal glucose levels for cells derived from embryos from normal pregnancies, or high glucose levels for cells derived from embryos from diabetic pregnancies. After these 6 passages, each cell line was split into low and high glucose containing media, regardless of origin. Thus, cells from 2 different metabolic conditions were adapted to two media conditions, respectively, so that in each subsequent assay, 4 conditions were compared. Figure 1 depicts a flow chart for the experimental design of this study. The first set of experiments measured the capacity of cells to migrate in different glucose concentration conditions after a wide scratch had been placed through the middle of a confluent cell layer in 24-well plates.

The net distance traveled by normal cells into the scratch was not different between conditions, regardless of the glucose concentration for the growth and maintenance, or the glucose concentration in the migration assay, respectively (Figure 2A). However, when cells from an embryo of a diabetic pregnancy (red bars) were tested in the same assay conditions on the same 24-well plate, cells migrated farther if they had been grown/maintained and assayed in low glucose medium compared to those same cells assayed in high glucose condition. Even less migration was observed from diabetes-exposed cells that were grown/maintained in high glucose medium: they migrated slower in low glucose assay condition, and even less migration was evident in high glucose assay condition (Figure 2A, closed red bars). Thus, cells that were diabetes-exposed during pregnancy were more responsive to glucose concentrations during maintenance and in assay than normal cells under those conditions.

This observation that differences in migratory capacity were attributable to exposure to maternal diabetes *in utero* prompted us to perform subsequent assays as comparisons between normal (N) and diabetes-exposed (DE) cell lines; in either low glucose or high glucose assay conditions. Separating the assay condition onto different 24-well plates allowed us to increase the number of plating replicates for each cell line. Figure 2B depicts the data from an individual assay in low glucose concentration, and Figure 2C displays the aggregate results from four independent repetitions of the same experiment. Although the absolute net distance traveled varied between repeat experiments, the reproducible trend was that cells maintained in high glucose migrate slower than those maintained in low glucose, and that diabetes-exposed cells migrate slower than normal cells, particularly when maintained in high glucose concentrations. Thus, cell migratory capacity is impaired by exposure to high glucose *in vitro* and by diabetes-exposure *in vivo*.

To determine the extent to which glucose concentration at the time of assay affects cell migration, we performed the same set of experiments in medium containing the high glucose concentration. The data from an individual experiment using the same cell lines as before are displayed in Figure 2D, with aggregate results from 4 independent experiments shown in Figure 2E. While the assays in high glucose concentration exhibited a trend towards farther overall distance traveled by normal cells compared to assays in low glucose, it has to be kept in mind that those assays were performed on different dates and plates. We therefore limit our conclusions to comparisons of cell migration on the same 24-well plate. Taken together, we reproducibly found that exposure to high glucose in the assay conditions or during maintenance had minimal effect on migratory behavior of normal cells, while exposure to high glucose in the maintenance media produced impairment in cell migration in those cells that had previously been exposed to hyperglycemic conditions *in vivo* in a diabetic pregnancy. Thus, exposure to high glucose *in vivo* and continued exposure to high glucose levels *in vitro* reduces the migratory capacity of primary embryo-derived cells.

Because the abovementioned experiments employed cell lines derived from a single pregnancy each, we sought to reproduce the findings with cells from independent pregnancies. We first compared the responses to assay conditions (Figure 3A), analogous to the experimental design shown in Figure 2. While in the particular experiment depicted, normal cells assayed in high glucose migrated faster than in a low glucose assay, this could

not be reproduced in three independent experiments with the same cells. There was also no difference in migratory capacity of diabetes-exposed cells that were maintained in low glucose concentrations when compared to normal cells. However, diabetes-exposed cells that were maintained in high glucose concentrations exhibited impaired migration, both when compared to the low glucose-maintained line, and when compared to normal cells maintained and assayed in high glucose conditions. Since a difference in migratory capacity between these two cell lines was reproducibly seen only in the high glucose concentration assay, additional experiments were conducted in high glucose concentration conditions (Figure 3B depicts results from an individual experiment and Figure 3C shows aggregate results from four independent experiments). Testing a third set of cell lines for migratory capacity did not produce differences to our earlier results (data not shown). The finding that combined exposure to high glucose in utero and in culture reduces migratory capacity was thus confirmed with several independent cell lines in multiple independent experiments.

Two-factor ANOVA analysis was performed to analyze the relative contribution of the two variables “*in vivo* exposure” and “glucose concentration in the maintenance media” on the ability of cells to migrate. In the experiments depicted in Figure 2, interactions between both factors were detected in the statistical analysis when migration was assayed in low glucose media ( $p=0.0003$ ) but not in high glucose conditions. Notably, “*in vivo* exposure” was the stronger factor over “glucose concentration in the maintenance media” (with “exposure” contributing 56.1% of the variation in Panel B and 27.8% in Panel C, and “glucose concentration” explaining 34.2% and 23.4%, respectively; all  $p$ -values  $<0.0001$ ). The finding of significant interactions was confirmed with the independent cell lines in Figure 3 ( $p=0.0004$  for Panel B,  $p<0.0001$  for Panel C). Again, “exposure” contributed to a greater extent than “glucose concentration” (with “exposure” explaining 30.6% and 27.8%, and “glucose concentration” explaining 23.2% and 23.4% of the variation, respectively). Thus, our finding of impaired migratory capacity is explained primarily by the prior *in vivo* exposure to maternal diabetes, with additional influence of the glucose concentration of the media in which cells were propagated in culture.

The apparent differences in migratory capacity could be associated with the cell density achieved in the assay plates after seeding and overnight incubation. Cell densities would differ by the time when the scratch is made, if the cell lines proliferated at different rates in high and low glucose-containing media. We therefore determined growth rates in different media over several days, as shown in Figure 4. The cell numbers for diabetes-exposed cells were significantly lower ( $P<0.05$ ) only at the 96-hour timepoint (4 days) when compared to normal cells in the same medium, but there were no differences at early time points. Importantly, there were no differences in the growth curves in the first 10–16 hours (overnight), excluding differential proliferation after seeding in the assay plate as a confounder for the migration assays. Consistency of seeding and confluence of the cultures prior to placing the scratch was also ascertained by visual inspection.

A plausible biological cause of impaired cell migration could be altered energy metabolism in conditions of excess glucose. Hyperglycemia-induced oxidative stress, as is present in diabetes-exposed embryos (Forsberg, Borg et al. 1996, Loeken 2005), may affect mitochondrial function and lead to reduced generation of energy, leaving less than required

for optimal cell migration. To test this proposition, we measured mitochondrial respiration in normal and diabetes-exposed cells using the Seahorse instrument. Figure 5 displays two independent experiments for two normal and two diabetes-exposed cell lines each, and additional repeat experiments yielded equivalent results (not shown). When normalized to the baseline value at 7 minutes, the curves for the cell lines produced the same patterns, irrespective of prior exposure *in vivo*. Oxygen consumption rates and reserve capacity did not differ between the cell lines, and neither did extracellular acidification rates (data not shown). Multiple repeat experiments comparing cells exposed to high or low glucose conditions during the assay in the Seahorse instrument (data not shown) also did not provide any evidence for altered metabolic activity by maintenance condition or prior exposure, at least according to parameters measured in the Seahorse instrument.

We then investigated the expression of nutrient transporters, with particular focus on glucose transporters (Figure 6), and, given that diabetes is associated with hyperlipidemia, on fatty acid transporters (Figure 7). Messenger RNA levels for several glucose transporters were undetectable (Slc2a2/Glut2) or very low (note that higher Ct values reflect lower expression levels), such as for Slc2a3/Glut3, Slc2a4/Glut4 and Slc2a7/Glut7, and moderately low expression was found for Slc2a6/Glut6, Slc2a8/Glut8, Slc2a9/Glut9, Slc2a12/Glut12, and Slc2a13/Glut13. The most strongly expressed glucose transporters in both normal and diabetes-exposed cells were Slc2a1/Glut1 and Slc2a10/Glut10 (note: lower Ct values signify higher relative expression levels). Expression levels for many of these genes were stable between passages 12 and 24 of cell culture, although some decreases were detected with time (significant changes indicated in blue), most notably for Slc2a1/Glut1, Slc2a3/Glut3, Slc2a5/Glut5 and Slc2a13/Glut13. The biological relevance of these changes in late-passage cells is currently unknown, as all migration assays were done with early passage cells.

Differences in transporter expression were detected when the same cell line was maintained in low and high glucose media in parallel (significant fold-changes indicated in green), but this was not observed for all genes or conditions. Most of the differences were found for normal cells, except for Slc2a5/Glut5 and Slc2a9/Glut9 at passage 12, when diabetes-exposed cells expressed these transporters at higher levels when cultured in high glucose media. While elevated expression of these transporters would enable the cells to utilize more of the available glucose, the metabolic assays do not provide evidence for increased metabolism, at least by the parameters measured in the Seahorse instrument.

Most relevant to the migratory impairments of diabetes-exposed cells would be differences in transporter expression associated with prior exposure *in vivo*. Lower expression in diabetes-exposed cells was detected for Slc2a1/Glut1 at passage 12, although at only a moderate fold-change of 1.2-fold. Decreased expression was also found for Slc2a5/Glut5, but given its low overall expression levels, the biological significance of this remains to be examined. Increased expression of Slc2a3/Glut3, Slc2a6/Glut6, Slc2a8/Glut8, Slc2a9/Glut9, Slc2a10/Glut10, Slc2a12/Glut12, and Slc2a13/Glut13 was measured in diabetes-exposed cells, albeit not at all time points or in all conditions. It is important to note here that the patterns of glucose transporter gene expression at passage 12 do not overtly correlate, neither directly nor inversely, with migratory capacity.

Largely similar interpretations pertain to the measurements of fatty acid transporter gene expression (Figure 7): Slc27a1/Fatp1, Slc27a3/Fatp3, Slc27a6/Fatp6 and Slc27a5/Fatp5 were expressed at decreasing levels relative to each other, and Slc27a4/Fatp4 had the highest expression level, but there were no differences by maintenance or exposure. CD36 and Slc27a2/Fatp2 were undetectable. Of the mitochondrial fatty acid transporters, Cpt1b had the lowest expression, and Cpt1a the highest level. Differences with potential to explain migratory impairments would be increased expression of Slc27a1/Fatp1 and Slc27a3/Fatp3 in diabetes-exposed cells maintained in high glucose, and reduced expression of Slc27a6/Fatp6 in diabetes-exposed cells, particularly when maintained in high glucose. Thus, these cells may be capable of metabolizing more fatty acids than normal cells. Yet, the mitochondrial activity measurements do not provide evidence for altered oxygen consumption in our cultured cells.

We also measured the expression of two genes known to be affected by oxidative stress, Gapdh and Gpx4 (Figure 8). No differences were found in the expression of Gapdh at passage 12, and only minor differences at passage 24 in diabetes-exposed cells. Gpx4 expression was higher in diabetes-exposed cells compared to normal, at passage 12 in cells maintained in low glucose, and at passage 24 in both maintenance conditions. The higher expression of Gpx4 in diabetes-exposed cells may indicate higher levels of oxidative stress, a possibility that remains to be investigated.

## Discussion

Migration of cells during mammalian gastrulation is critical to formation of tissues and organs, and perturbations of cell migration can cause structural defects, such as heart defects, skeletal anomalies, and neural tube closure defects. Such birth defects are more frequent in progeny from pregnancies affected by maternal diabetes (Mills, Baker et al. 1979, Martinez-Frias 1994). We have previously shown that exposure of mouse embryos to the diabetic maternal environment is associated with impaired cell migration during gastrulation, prior to neural tube closure (Salbaum, Kruger et al. 2015). Specifically, we demonstrated that diabetes-exposed embryos manifested protrusions in the primitive streak that consisted of accumulations of mesodermal cells. Explant cultures of primitive streak tissue, and of the accumulations that form the protrusions, showed that migration of mesodermal cells was impaired in diabetes-exposed embryonic tissue. In order to investigate molecular mechanisms underlying impaired mesodermal cell migration *in vivo*, we sought to establish an *in vitro* system that mimics this process.

We here report isolation of embryonic cell lines from diabetes-affected pregnancies of the non-obese diabetic (NOD) strain of mice. These primary cells exhibit mesenchymal and fibroblast-like appearance and thus can be assumed to be of mesodermal origin, and expression of mesodermal markers was detected (unpublished results). Assays for cell migratory capacity in the classical monolayer ‘wound scratch’ paradigm (Lampugnani 1999) revealed that cells isolated from embryos exposed to maternal diabetes *in vivo* migrated slower and traveled shorter distances into the scratch area, when compared to cells isolated from embryos of normal pregnancies. Thus, these cell lines reproduced the migration impairment *ex vivo*, in primary cell culture. Diabetes-exposed cells exhibited impaired cell

migration particularly when cultured in media containing high concentrations of glucose, simulating the hyperglycemic *in vivo* situation. These results show that even after isolation and passaging in cell culture, diabetes-exposed embryonic cells retained a “memory” of the *in vivo* exposure, and they reproduced the finding of diminished migratory capacity. Intriguingly, this “memory” appears to be maintained in diabetes-exposed embryos long after mesoderm formation, as the cells for our primary cultures were isolated from E12.5 embryos. We therefore consider the migratory impairment we observed in our new cell lines as an *in vitro* model of impaired mesodermal cell migration.

Reduced migratory capacity was also reported for neural crest cells derived from diabetes-exposed rat embryos (Suzuki, Svensson et al. 1996), leading these authors to conclude that *in vivo* exposure to maternal diabetes “permanently influences” the future phenotype of neural crest-derived cells. Similar to our findings, the impairment in neural crest cell migratory capacity was exaggerated by culture of these cells in high glucose concentrations *in vitro*. Taken together with our previous findings of impaired mesoderm in diabetes-exposed embryos *in vivo* (Salbaum, Kruger et al. 2015), the present study thus implicates impairments of cell migratory capacity as a common biological response to maternal diabetes in two cell lineages of different developmental origin. It remains to be investigated whether additional embryonic cell lineages in the diabetic pregnancy paradigm are affected by impairments in their migratory capacity.

We then attempted to define molecular correlates for this cellular phenotype, by investigating growth properties, energy metabolism and gene expression in these cells. The latter experiments focused on glucose and fatty acid transporters, because in the mouse diabetic pregnancies are characterized by severe hyperglycemia (Kappen, Kruger et al. 2011), and accompanied by hyperlipidemia in humans and rodents (Hollingsworth and Grundy 1982, Damasceno, Volpato et al. 2002), including mice (our own unpublished results). Altered nutrient utilization and altered energy metabolism could provide plausible explanations for the impaired migratory capacity of diabetes-exposed cells. Growth curves did not differ between exposed and normal cells in the short time frames of typical cell passaging and culture/seeding before metabolic measurements and migration assays. Likewise, there were no significant differences in metabolic capacity between exposed and normal cells, irrespective of the concentration of glucose offered in the assay (data not shown). Although we did not specifically test for utilization of other nutrients, the metabolic assays did not provide evidence for reduced energy (ATP-) production in diabetes-exposed cells. Thus, we consider it unlikely that energetic perturbation could be involved to explain the phenotype of impaired cell migration.

Gene expression levels were remarkably stable over time in culture for many of the glucose and fatty acid transporters examined. Glucose level in culture, and even exposure to diabetes *in vivo* did not substantially affect expression of any of these genes. Notable exceptions were Slc2a1/Glut1, Slc2a5/Glut5 and Slc2a6/Glut6, where diabetes-exposure was associated with reduced expression at early passage, while for Slc2a3/Glut3 and Slc2a9/Glut9, expression was increased by exposure. It has to be kept in mind, however, that differences were moderate (below 2-fold) and that most glucose transporter family members were expressed only at very low levels. Overall, Slc2a1/Glut1 appears to be the dominant glucose

transporter in these cells, followed by Slc2a10/Glut10. In contrast to reports implicating Glut2 in diabetes-exposed embryos (Li, Thorens et al. 2007), cells derived from such embryos did not exhibit any measurable expression of Slc2a2/Glut2 in our assays. We currently do not know if Glut2 is expressed at the time of cell isolation and then lost during culture, or whether the isolated cells already lacked Glut2 expression in the embryo.

The dominant cell surface fatty acid transporter in these cells appeared to be Slc27a4/Fatp4, followed by Slc27a1/Fatp1 and Slc27a3/Fatp3. Some variability of expression was observed for Slc27a1/Fatp1 by time, glucose level in culture and diabetes exposure, but only in late passage cells. The mitochondrial fatty acid transporters Cpt1 and 2 were expressed, with isoform Cpt1a at highest level, but differences were only observed in late passage cells. Considering that neither ATP-production nor oxygen consumption were altered in diabetes-exposed cells, it remains to be investigated to what extent nutrient utilization and cellular energy metabolism could be affected by the observed changes in gene expression levels. Uniform expression of Gapdh would also be consistent with the interpretation of normal metabolic activity in all cell lines tested. *In vivo*, Gapdh expression is reduced in diabetes-exposed embryos (Wentzel, Ejdesjo et al. 2003, Pavlinkova, Salbaum et al. 2009), which might be responsible for the lower rate of glycolysis and ATP production observed in exposed embryos (Zhao, Hakvoort et al. 2016). To what extent or how our embryo-derived primary cells normalize their expression of Gapdh, and ATP production, after the *in vivo* exposure is currently unknown.

Of interest is that expression of Gpx4 was higher in cells derived from embryos that were exposed to diabetes *in vivo*, although the difference to normal cells did not reach statistical significance when cells were maintained in high glucose-conditioning media. Gpx4 activity is the only anti-oxidant capacity that cannot be ablated from embryonic cells without compromising survival (Yant, Ran et al. 2003, Liang, Yoo et al. 2009), indicating that the lipid-peroxide-neutralizing action of Gpx4 is essential. Increased Gpx4 expression levels thus might be an indicator of elevated phospholipid hydroperoxide production in diabetes-exposed cells. Gpx4 has been shown to interfere with Wnt-signaling in zebrafish through physical interaction with the TCF/Lef transcription factor complex (Rong, Zhou et al. 2017). Mouse mutants for Wnt-signaling pathway components Wnt3, Lrp5/6,  $\beta$ -catenin and Tcf3 also exhibit cell migration defects during gastrulation (reviewed in (Herion, Salbaum et al. 2014), suggesting that Gpx4 modulation of this pathway could play a role in the migration defects of diabetes-exposed cells. Consistent with this possibility is our previous finding of reduced Wnt3a expression in diabetes-exposed embryos (Pavlinkova, Salbaum et al. 2008). Expression profiling of diabetes-exposed embryos at E8.5 and E10.5 did not reveal differences in Gpx4 at the mRNA level (unpublished observations), but measurements of Gpx4 protein activity, especially in the NOD mouse model, have yet to be performed.

Hyperglycemia has previously been shown to inhibit the migration of Schwann cells out of cultured mouse dorsal root ganglia (Gumy, Bampton et al. 2008). Reduced migration of fibroblasts isolated from db/db (Leptin-receptor-deficient) mice was observed after onset of diabetes (Lerman, Galiano et al. 2003), and this was associated with increased production of matrix metalloproteinase MMP9, which is known to be localized at the leading edge of migrating cells (Sivak, West-Mays et al. 2004, Mauris, Woodward et al. 2014). The leading

edge also contains the WAVE complex, a regulator of the actin skeleton. Absence of WAVE was shown to be associated with impaired migration of mesodermal cells during gastrulation, leading to neural tube and heart defects in mouse mutants lacking the regulatory component of the WAVE complex Nap1 (Rakeman and Anderson 2006). The WAVE complex is under control of the GTPase Rac1; interestingly, mouse mutants with deletion of Rac1 in epiblast cells exhibit impaired migration of mesodermal cells (Migeotte, Grego-Bessa et al. 2011), similar to NOD mouse embryos exposed to maternal diabetes (Salbaum, Kruger et al. 2015). Thus, it is possible that the adverse effects of maternal diabetes on mesodermal cell migration in vivo and mesoderm-derived primary fibroblast cell migration in vitro could be mediated by pathways previously identified in genetic ablation approaches in mouse mutants (Herion, Salbaum et al. 2014).

Another mechanism that regulates cell motility is based upon phosphorylation of Vimentin by Akt kinase, and Vimentin stability is dependent on Akt activity (Zhu, Rosenblatt et al. 2011). We have recently shown that the embryonic cells affected by diabetes-induced impairment in migration express Vimentin when placed into explant cultures (Salbaum, Kruger et al. 2015). Constitutively active Akt can induce cell migration in otherwise immotile mesenchymal cells (Ackah, Yu et al. 2005), suggesting the possibility that impaired migration in our cultures could be associated with reduced Vimentin phosphorylation and reduced Akt activity.

Also relevant to the speed of cell migration is the extent of cell adhesion (Burdal, Damsky et al. 1993, Hammerschmidt and Wedlich 2008). While our comparisons of diabetes-exposed to normal cells were conducted on standard gelatin-coated plates, there is evidence that the extracellular matrix composition in diabetes-exposed embryos is altered by the exposure (Cagliero, Forsberg et al. 1993). Altered ECM composition would be expected to affect cell migration in cultures of embryo tissue explants, and early in the culture of primary cells, but it is unlikely to be maintained after extended cell passaging, as new extracellular matrix is produced. Yet, we cannot exclude the possibility that diabetes-exposed cells permanently change their repertoire of expression of ECM components after exposure. Investigations to distinguish between the various scenarios and to define the epigenetic basis for the “memory of exposure” in embryo-derived primary cells are currently underway.

Finally, our experiments show that maintaining normal primary cells in hyperglycemia-mimicking high glucose concentrations alone -even for extended amounts of time- is not sufficient to induce migratory impairment. Thus, the *in vivo* exposure -although its physiological hallmark is hyperglycemia- likely involves additional pathways that impinge on cell migratory capacity. Noteworthy in this regard are reports showing that components in the serum of diabetic dams can contribute to abnormalities in cultured embryos (Sadler 1980, Sadler, Phillips et al. 1986, Sadler, Hunter et al. 1989, Styrod and Eriksson 1992, Wentzel and Eriksson 1996). The new cell lines we have established will facilitate identification of such factors, and of the molecular basis for impaired cell migration, in the genetic context of the non-obese (NOD) mouse strain that is high susceptible to diabetes-induced neural-tube defects.

## Acknowledgements

We thank Dr. Krisztian Stadler for advice with the Seahorse measurements, Jennifer Martin for animal husbandry, Alexis Allen for imaging help, Dr. Robbie Beyl for advice on statistics, and Nancy Pease for administrative support. This work was funded in part by grants from the Eunice Kennedy Shriver National Institute of Child Health and Human Development (R01-HD086604, and R01-HD085017). The Cell Biology and Bioimaging Core and the Genomics Core at Pennington Biomedical Research Center are funded in part through the Nutrition and Obesity Research Center (P30-DK072476) and Center of Biomedical Research Excellence (P30-GM118430) grants from the National Institutes of Health. Claudia Kappen was also supported by the Peggy M. Pennington Cole Endowed Chair in Maternal Biology.

## References

- Ackah E, Yu J, Zoellner S, Iwakiri Y, Skurk C, Shibata R, Ouchi N, Easton RM, Galasso G, Birnbaum MJ, Walsh K and Sessa WC (2005). "Akt1/protein kinase Balpha is critical for ischemic and VEGF-mediated angiogenesis." *J Clin Invest* 115(8): 2119–2127. [PubMed: 16075056]
- Burdsal CA, Damsky CH and Pedersen RA (1993). "The role of E-cadherin and integrins in mesoderm differentiation and migration at the mammalian primitive streak." *Development* 118(3): 829–844. [PubMed: 7521282]
- Cagliero E, Forsberg H, Sala R, Lorenzi M and Eriksson UJ (1993). "Maternal diabetes induces increased expression of extracellular matrix components in rat embryos." *Diabetes* 42(7): 975–980. [PubMed: 7685721]
- Damasceno DC, Volpato GT, de I Paranhos Calderon Mattos and Rudge M. V. Cunha (2002). "Oxidative stress and diabetes in pregnant rats." *Anim Reprod Sci* 72(3–4): 235–244. [PubMed: 12137985]
- Forsberg H, Borg LA, Cagliero E and Eriksson UJ (1996). "Altered levels of scavenging enzymes in embryos subjected to a diabetic environment." *Free Radic Res* 24(6): 451–459. [PubMed: 8804988]
- Gumy LF, Bampton ET and Tolkovsky AM (2008). "Hyperglycaemia inhibits Schwann cell proliferation and migration and restricts regeneration of axons and Schwann cells from adult murine DRG." *Mol Cell Neurosci* 37(2): 298–311. [PubMed: 18024075]
- Hammerschmidt M and Wedlich D (2008). "Regulated adhesion as a driving force of gastrulation movements." *Development* 135(22): 3625–3641. [PubMed: 18952908]
- Harris MJ and Juriloff DM (2010). "An update to the list of mouse mutants with neural tube closure defects and advances toward a complete genetic perspective of neural tube closure." *Birth Defects Res A Clin Mol Teratol* 88(8): 653–669. [PubMed: 20740593]
- Herion NJ, Salbaum JM and Kappen C (2014). "Traffic jam in the primitive streak: the role of defective mesoderm migration in birth defects." *Birth Defects Res A Clin Mol Teratol* 100(8): 608–622. [PubMed: 25115487]
- Hollingsworth DR and Grundy SM (1982). "Pregnancy-associated hypertriglyceridemia in normal and diabetic women. Differences in insulin-dependent, non-insulin-dependent, and gestational diabetes." *Diabetes* 31(12): 1092–1097. [PubMed: 6757021]
- Juriloff DM and Harris MJ (2000). "Mouse models for neural tube closure defects." *Hum Mol Genet* 9(6): 993–1000. [PubMed: 10767323]
- Kappen C, Kruger C, MacGowan J and Salbaum JM (2011). "Maternal diet modulates the risk for neural tube defects in a mouse model of diabetic pregnancy." *Reprod Toxicol* 31(1): 41–49. [PubMed: 20868740]
- Kousseff BG (1999). "Diabetic embryopathy." *Curr Opin Pediatr* 11(4): 348–352. [PubMed: 10439209]
- Kruger C and Kappen C (2010). "Expression of cartilage developmental genes in Hoxc8- and Hoxd4-transgenic mice." *PLoS One* 5(2): e8978. [PubMed: 20126390]
- Kucera J (1971). "Rate and type of congenital anomalies among offspring of diabetic women." *J Reprod Med* 7(2): 73–82. [PubMed: 5095696]
- Lampugnani MG (1999). "Cell migration into a wounded area in vitro." *Methods Mol Biol* 96: 177–182. [PubMed: 10098136]

- Lerman OZ, Galiano RD, Armour M, Levine JP and Gurtner GC (2003). "Cellular dysfunction in the diabetic fibroblast: impairment in migration, vascular endothelial growth factor production, and response to hypoxia." *Am J Pathol* 162(1): 303–312. [PubMed: 12507913]
- Li R, Thorens B and Loeken MR (2007). "Expression of the gene encoding the high-Km glucose transporter 2 by the early postimplantation mouse embryo is essential for neural tube defects associated with diabetic embryopathy." *Diabetologia* 50(3): 682–689. [PubMed: 17235524]
- Liang H, Yoo SE, Na R, Walter CA, Richardson A and Ran Q (2009). "Short form glutathione peroxidase 4 is the essential isoform required for survival and somatic mitochondrial functions." *J Biol Chem* 284(45): 30836–30844. [PubMed: 19744930]
- Loeken MR (2005). "Current perspectives on the causes of neural tube defects resulting from diabetic pregnancy." *Am J Med Genet C Semin Med Genet* 135C(1): 77–87. [PubMed: 15800853]
- Martinez-Frias ML (1994). "Epidemiological analysis of outcomes of pregnancy in diabetic mothers: identification of the most characteristic and most frequent congenital anomalies." *Am J Med Genet* 51(2): 108–113. [PubMed: 8092185]
- Mauris J, Woodward AM, Cao Z, Panjwani N and Argueso P (2014). "Molecular basis for MMP9 induction and disruption of epithelial cell-cell contacts by galectin-3." *J Cell Sci* 127(Pt 14): 3141–3148. [PubMed: 24829150]
- Migeotte I, Grego-Bessa J and Anderson KV (2011). "Rac1 mediates morphogenetic responses to intercellular signals in the gastrulating mouse embryo." *Development* 138(14): 3011–3020. [PubMed: 21693517]
- Mills JL, Baker L and Goldman AS (1979). "Malformations in infants of diabetic mothers occur before the seventh gestational week. Implications for treatment." *Diabetes* 28(4): 292–293. [PubMed: 437367]
- Ornoy A, Reece EA, Pavlinkova G, Kappen C and Miller RK (2015). "Effect of maternal diabetes on the embryo, fetus, and children: congenital anomalies, genetic and epigenetic changes and developmental outcomes." *Birth Defects Res C Embryo Today* 105(1): 53–72. [PubMed: 25783684]
- Otani H, Tanaka O, Tawaki R, Naora H and Yoneyama T (1991). "Diabetic environment and genetic predisposition as causes of congenital malformations in NOD mouse embryos." *Diabetes* 40(10): 1245–1250. [PubMed: 1936588]
- Pavlinkova G, Salbaum JM and Kappen C (2008). "Wnt signaling in caudal dysgenesis and diabetic embryopathy." *Birth Defects Res A Clin Mol Teratol* 82(10): 710–719. [PubMed: 18937363]
- Pavlinkova G, Salbaum JM and Kappen C (2009). "Maternal diabetes alters transcriptional programs in the developing embryo." *BMC Genomics* 10: 274. [PubMed: 19538749]
- Rakeman AS and Anderson KV (2006). "Axis specification and morphogenesis in the mouse embryo require Nap1, a regulator of WAVE-mediated actin branching." *Development* 133(16): 3075–3083. [PubMed: 16831833]
- Robertson EJ (1987). "Embryo-derived stem cell lines" In: *Teratocarcinomas and embryonic stem cells, a practical approach*, Robertson EJ, ed. IRL Practical Series, Oxford University Press, Oxford, New York, Tokyo: 71–112.
- Rong X, Zhou Y, Liu Y, Zhao B, Wang B, Wang C, Gong X, Tang P, Lu L, Li Y, Zhao C and Zhou J (2017). "Glutathione peroxidase 4 inhibits Wnt/beta-catenin signaling and regulates dorsal organizer formation in zebrafish embryos." *Development* 144(9): 1687–1697. [PubMed: 28302747]
- Sadler TW (1980). "Effects of maternal diabetes on early embryogenesis: I. The teratogenic potential of diabetic serum." *Teratology* 21(3): 339–347. [PubMed: 7455923]
- Sadler TW, Hunter ES 3rd, Wynn RE and Phillips LS (1989). "Evidence for multifactorial origin of diabetes-induced embryopathies." *Diabetes* 38(1): 70–74. [PubMed: 2909414]
- Sadler TW, Phillips LS, Balkan W and Goldstein S (1986). "Somatomedin inhibitors from diabetic rat serum alter growth and development of mouse embryos in culture." *Diabetes* 35(8): 861–865. [PubMed: 3732629]
- Salbaum JM and Kappen C (2010). "Neural tube defect genes and maternal diabetes during pregnancy." *Birth Defects Res A Clin Mol Teratol* 88(8): 601–611. [PubMed: 20564432]

- Salbaum JM, Kruger C, MacGowan J, Herion NJ, Burk D and Kappen C (2015). "Novel Mode of Defective Neural Tube Closure in the Non-Obese Diabetic (NOD) Mouse Strain." *Sci Rep* 5: 16917. [PubMed: 26593875]
- Sivak JM, West-Mays JA, Yee A, Williams T and Fini ME (2004). "Transcription Factors Pax6 and AP-2alpha Interact To Coordinate Corneal Epithelial Repair by Controlling Expression of Matrix Metalloproteinase Gelatinase B." *Mol Cell Biol* 24(1): 245–257. [PubMed: 14673159]
- Styraud J and Eriksson UJ (1992). "Development of rat embryos in culture media containing different concentrations of normal and diabetic rat serum." *Teratology* 46(5): 473–483. [PubMed: 1462252]
- Suzuki N, Svensson K and Eriksson UJ (1996). "High glucose concentration inhibits migration of rat cranial neural crest cells in vitro." *Diabetologia* 39(4): 401–411. [PubMed: 8777989]
- Wentzel P, Ejdesjo A and Eriksson UJ (2003). "Maternal diabetes in vivo and high glucose in vitro diminish GAPDH activity in rat embryos." *Diabetes* 52(5): 1222–1228. [PubMed: 12716756]
- Wentzel P and Eriksson UJ (1996). "Insulin treatment fails to abolish the teratogenic potential of serum from diabetic rats." *Eur J Endocrinol* 134(4): 459–466. [PubMed: 8640298]
- Yant LJ, Ran Q, Rao L, Van Remmen H, Shibatani T, Belter JG, Motta L, Richardson A and Prolla TA (2003). "The selenoprotein GPX4 is essential for mouse development and protects from radiation and oxidative damage insults." *Free Radic Biol Med* 34(4): 496–502. [PubMed: 12566075]
- Zhao J, Hakvoort TB, Willemsen AM, Jongejan A, Sokolovic M, Bradley EJ, de Boer VC, Baas F, van Kampen AH and Lamers WH (2016). "Effect of Hyperglycemia on Gene Expression during Early Organogenesis in Mice." *PLoS One* 11(7): e0158035. [PubMed: 27433804]
- Zhu QS, Rosenblatt K, Huang KL, Lahat G, Brobey R, Bolshakov S, Nguyen T, Ding Z, Belousov R, Bill K, Luo X, Lazar A, Dicker A, Mills GB, Hung MC and Lev D (2011). "Vimentin is a novel AKT1 target mediating motility and invasion." *Oncogene* 30(4): 457–470. [PubMed: 20856200]

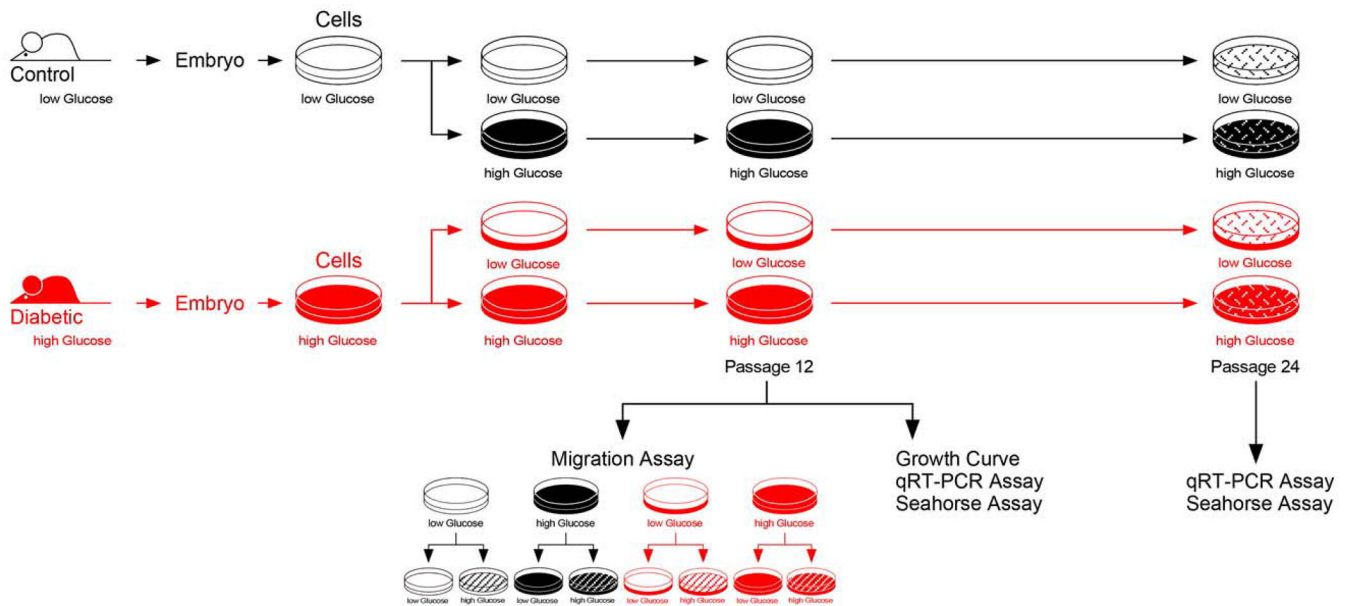


### Figure 1. Schematic Depiction of Experimental Design.

Using the NOD mouse model, primary cells were isolated from embryos of normal and diabetic pregnancies. Cells were kept in culture medium with a glucose concentration designed to reflect the *in vivo* conditions of low glucose level (normal cells) and high glucose level (cells from diabetes-exposed embryos), respectively. After 6 Passages, half of each cell line was transferred into medium with the other glucose concentration, grown for 3 more Passages and frozen in multiple aliquots at Passage 9. For each assay, aliquots were thawed, and cells propagated in the respective medium until assay. In the migration assays, conditions of either high or low glucose in the assay were applied, resulting in 8 experimental groups.

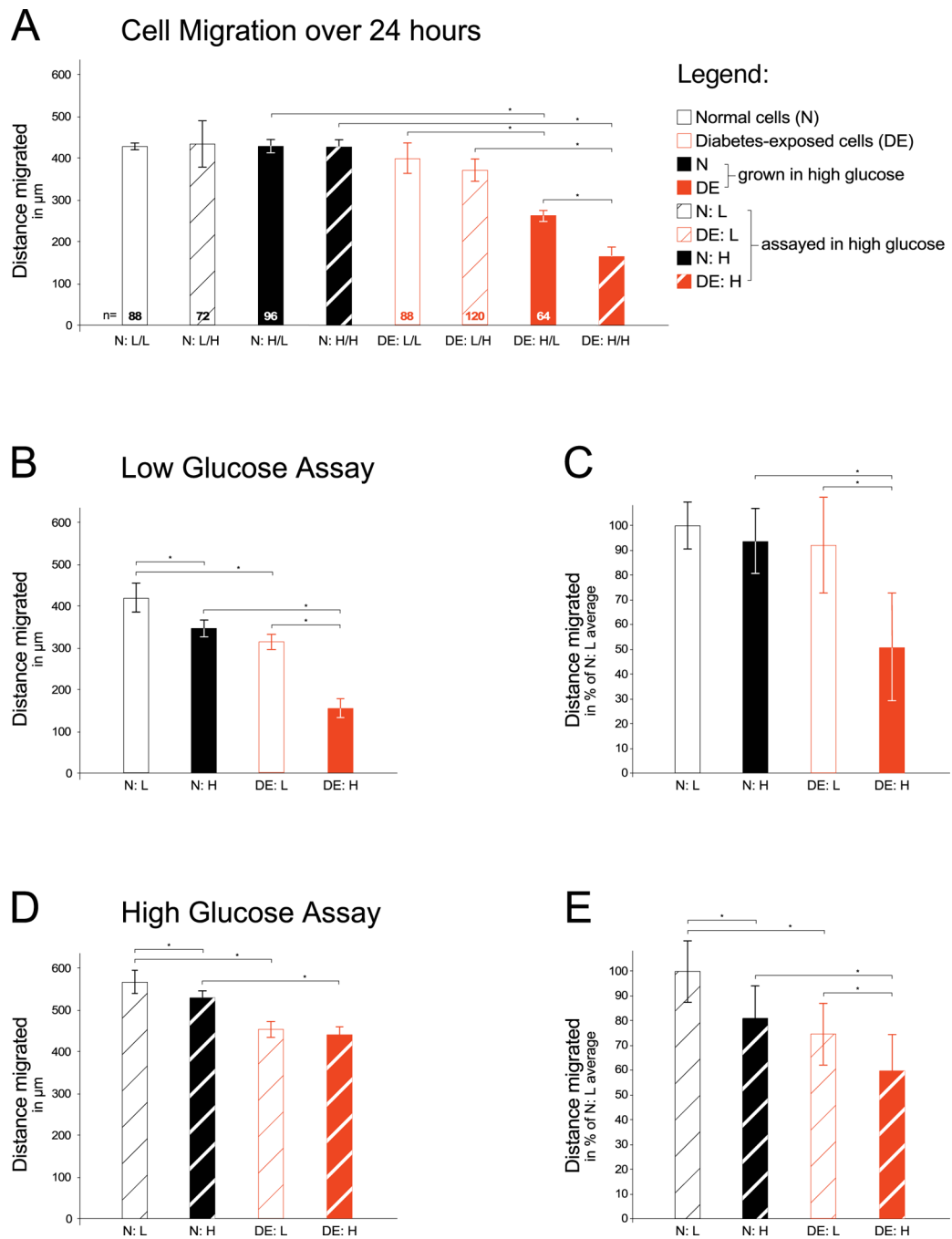


**Figure 2. Assay for migratory capacity of primary embryonic fibroblasts exposed to maternal diabetes *in vivo*.**

Primary cells were isolated from embryos of either normal (N) pregnancies or diabetic (DE) pregnancies as described in the Methods section. For each migration assay, isolates were thawed and grown for 2–3 passages before the assay in either low (L) glucose conditions or high (H) glucose-containing media. Migration assays were performed in either media condition as indicated. Panel A: A scratch was made through the confluent cell layer, and time-lapse images were taken of cells migrating into the scratch over the next 24 hours (number of wells/condition = 3, number of cells measured/condition is given at the bottom

of each bar). Cells that came from diabetes-exposed embryos migrated shorter distances, particularly after having been maintained in high glucose conditions. Panel B: Individual experiment with all four conditions assayed on the same 24-well plate. For condition N:L migration distance was measured for a total of 125 individual cells (25 cells in one well and 20 cells in each of 5 wells); for N:H 130 individual cells were measured (17, 19, 35, 19, 20, and 20 cells/well); for condition D:L 133 individual cells were measured (19, 21, 20, 20, 30, and 23 cells/well); and for condition D:H 79 individual cells were measured from 4 wells (19, 26, 18, and 19 cells/well). Panel C: Aggregate results from four independent experiments, in which the average of condition N:L was normalized to 100%, and individual well averages were transformed to percentage values relative to the 100% for each experiment, respectively. Condition N:L was represented by a total of 21 wells, and migration distance was measured for a total of 642 individual cells; for condition N:H 670 individual cells were measured; for condition D:L 762 individual cells were measured; and for condition D:H 350 individual cells were measured from 15 wells. The averages were calculated over all wells for a given condition (21, 21, 21, and 15 wells/condition, respectively). Panel D: Individual experiment with 6 wells/condition, migration assayed in high glucose-containing media. For condition N:L migration distance was measured for a total of 168 individual cells, from 36, 31, 38, 18, 24, and 21 cells/well, respectively; for N:H 190 individual cells were measured (37, 40, 35, 25, 24, and 29 cells/well); for condition D:L 180 individual cells were measured (34, 40, 41, 24, 22, and 19 cells/well); and for condition D:H 113 individual cells were measured (24, 26, 11, 18, 16, and 18 cells/well). Panel E: Aggregate results from four independent experiments, normalized as described for Panel C. Condition N:L was represented by a total of 21 wells, and migration distance was measured for a total of 275 individual cells; for condition N:H 356 individual cells were measured; for condition D:L 386 individual cells were measured; and for condition D:H 179 individual cells were measured from 13 wells. The average was calculated over all wells for a given condition (21, 21, 21, and 13 wells/condition, respectively). Significantly ( $P < 0.05$ ) reduced cell migratory capacity (indicated by asterisks) was observed in cells with prior exposure to maternal diabetes *in vivo*, particularly when these cells were maintained in high glucose-containing media.

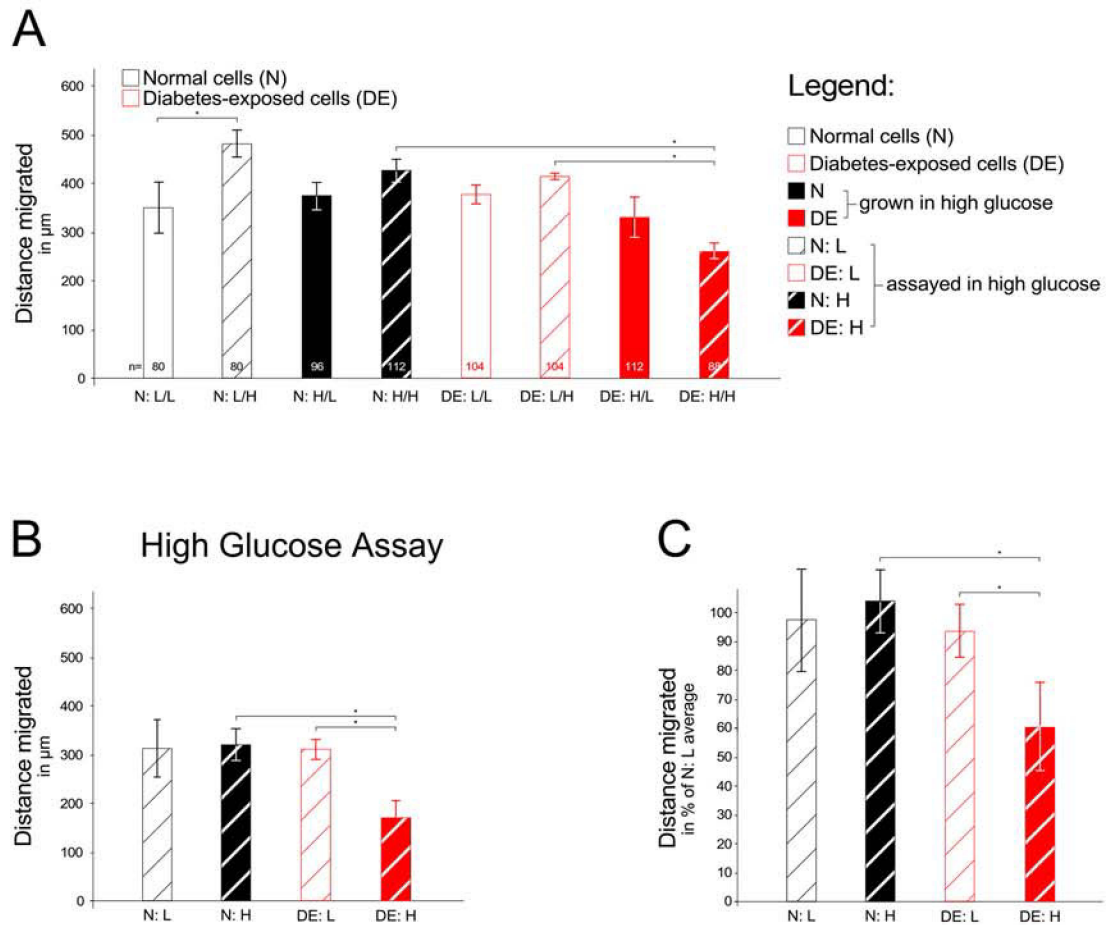


**Figure 3. Migratory capacity of additional independent primary embryonic cell lines.**

Cell migration was measured as described in the Legend to Figure 2. Panel A: Assay over the 24 hours (number of wells/condition = 3). Panel B: Individual experiment with all four conditions on the same 24-well plate, assayed in high glucose-containing media. For condition N:L migration distance was measured for a total of 200 individual cells (40, 32, 24, 24, 40, and 40 cells/well); for N:H 216 individual cells were measured (32, 16, 48, 32, 48, and 40 cells/well); for condition D:L 240 individual cells were measured (56, 32, 40, 40, 40, and 32 cells/well); and for condition D:H 174 individual cells were measured from 4 wells (47, 47, 40, and 40 cells/well). Panel C: Aggregate results from four independent experiments. Over all four experiments, condition N:L was represented by a total of 18 wells, and migration distance was measured for a total of 553 individual cells; for condition N:H 679 individual cells were measured (18 wells); for condition D:L 669 individual cells were measured (18 wells); and for condition D:H 566 individual cells were measured from 15 wells. Cells with prior exposure to maternal diabetes *in vivo* exhibited significantly ( $P < 0.05$ ) reduced cell migratory capacity when these cells were maintained in high glucose-containing media.

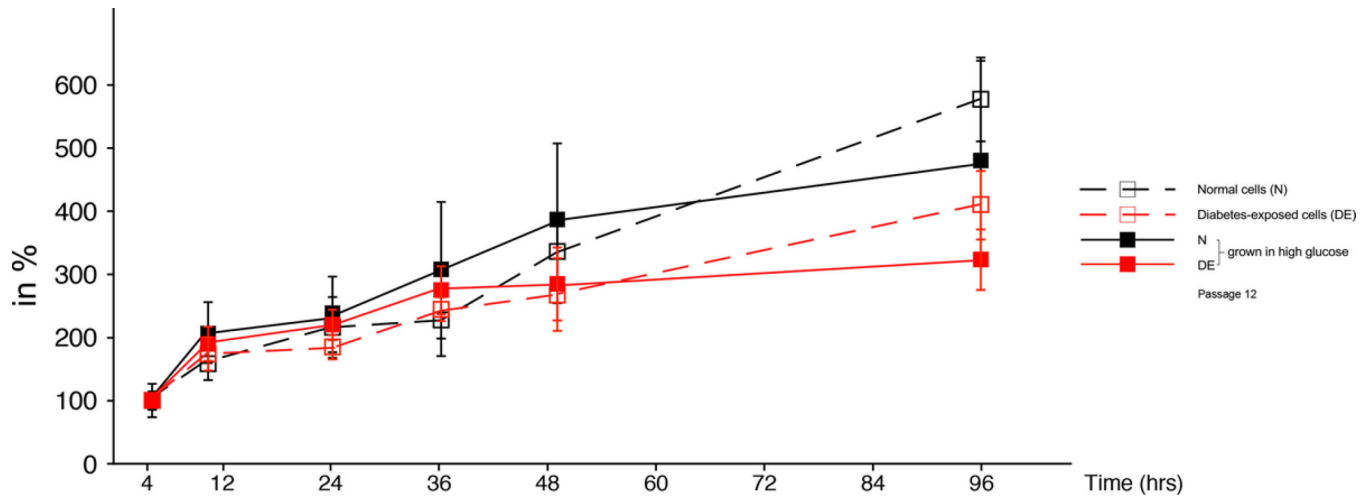


**Figure 4. Cell counting of primary embryonic cells in culture.**

The same cell lines as used in Figure 3 were assayed for cell number (for experimental details see Methods section), and were maintained and assayed (triplicate wells/condition and time point) in low glucose conditions (open symbols, hatched lines), or high glucose conditions (closed symbols, solid lines). Significant differences ( $P < 0.05$ ) were only found between normal and diabetes-exposed cells in each condition at 96 hours.

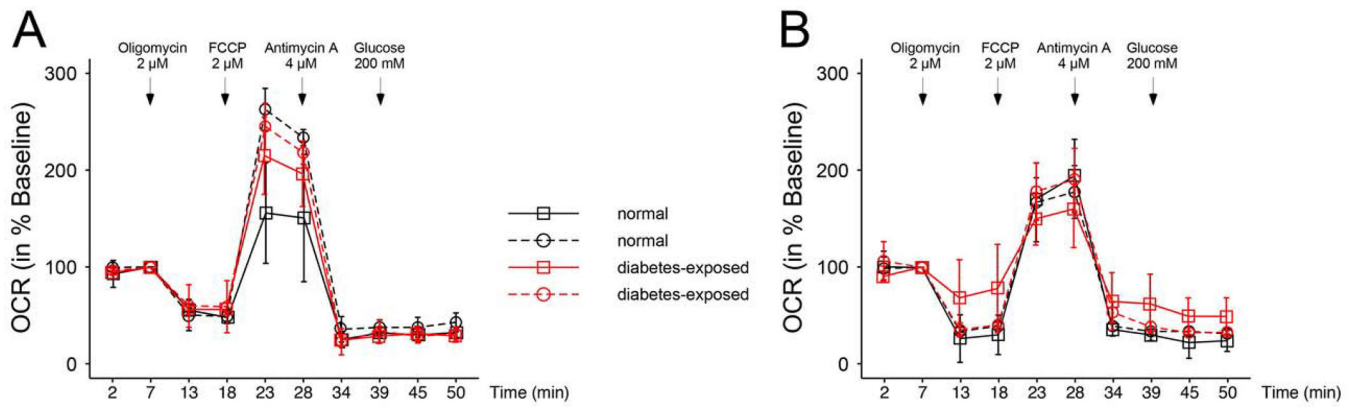


**Figure 5. Measurements of cellular energy metabolism in the Seahorse instrument.**

The assays were performed in quadruplicate wells/cell line, comparing the oxygen consumption rates of cell lines used in Figure 2 (round symbols, hatched lines) and Figure 3 (square symbols, solid lines). The addition of compounds is depicted by arrows, and cells had been maintained in high glucose media before the assays. Panels A and B display results from two independent experiments.

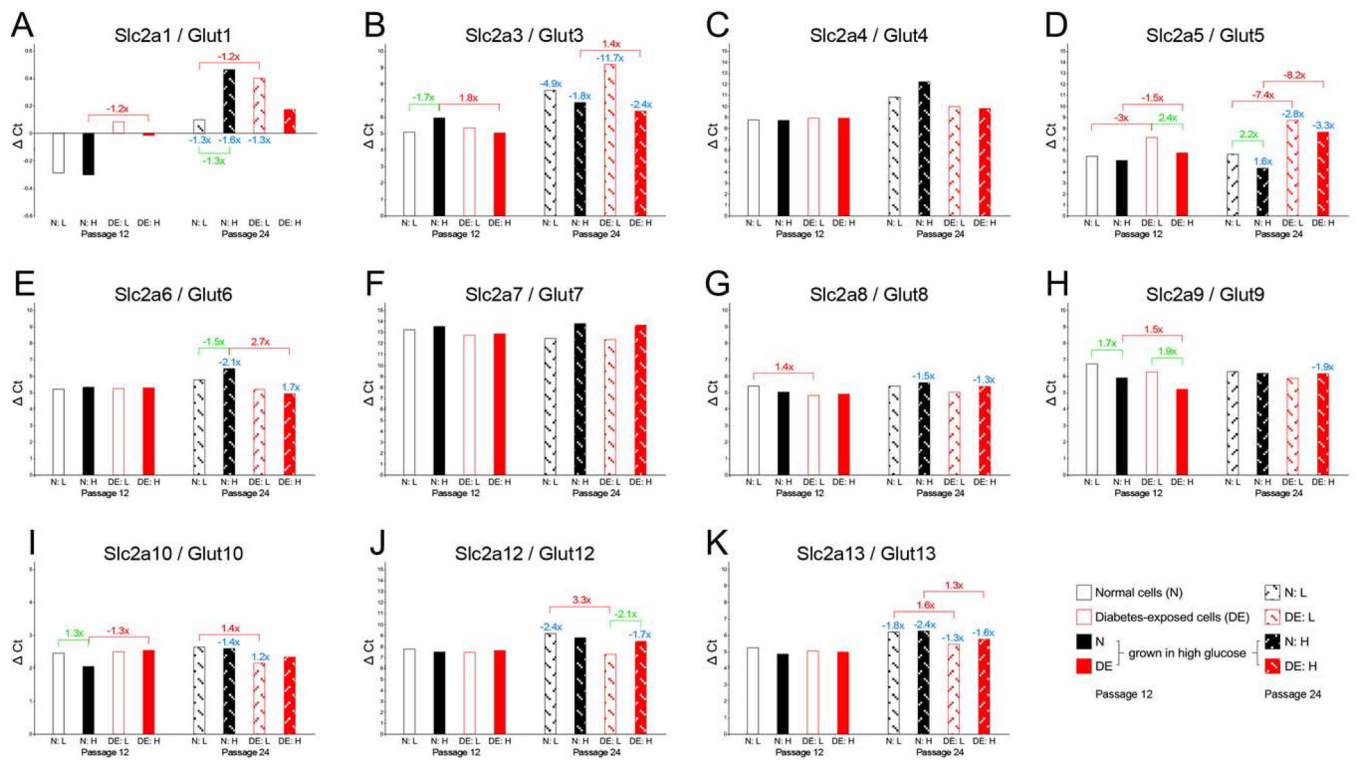


**Figure 6. Expression of nutrient transporters as assayed by quantitative real-time PCR: glucose transporters**  
 Expression levels are expressed in Cycle threshold (Ct) values, relative to the references gene averages (see Methods for details), with each sample measured in triplicate on the same assay plate. Standard deviations for the technical replicates are not depicted because they were negligible. Higher bars (larger Ct values) correspond to lower expression levels, smaller Ct values (lower bars) reflect higher expression levels. Fold-changes are given for significant differences in expression level when compared for the same condition between passage 12 and passage 24 (blue numbers), for comparisons of the same cell line in different maintenance media conditions (green numbers), and for differences between normal and diabetes-exposed cells (red numbers). Note that Y-axes have different scales for different genes.

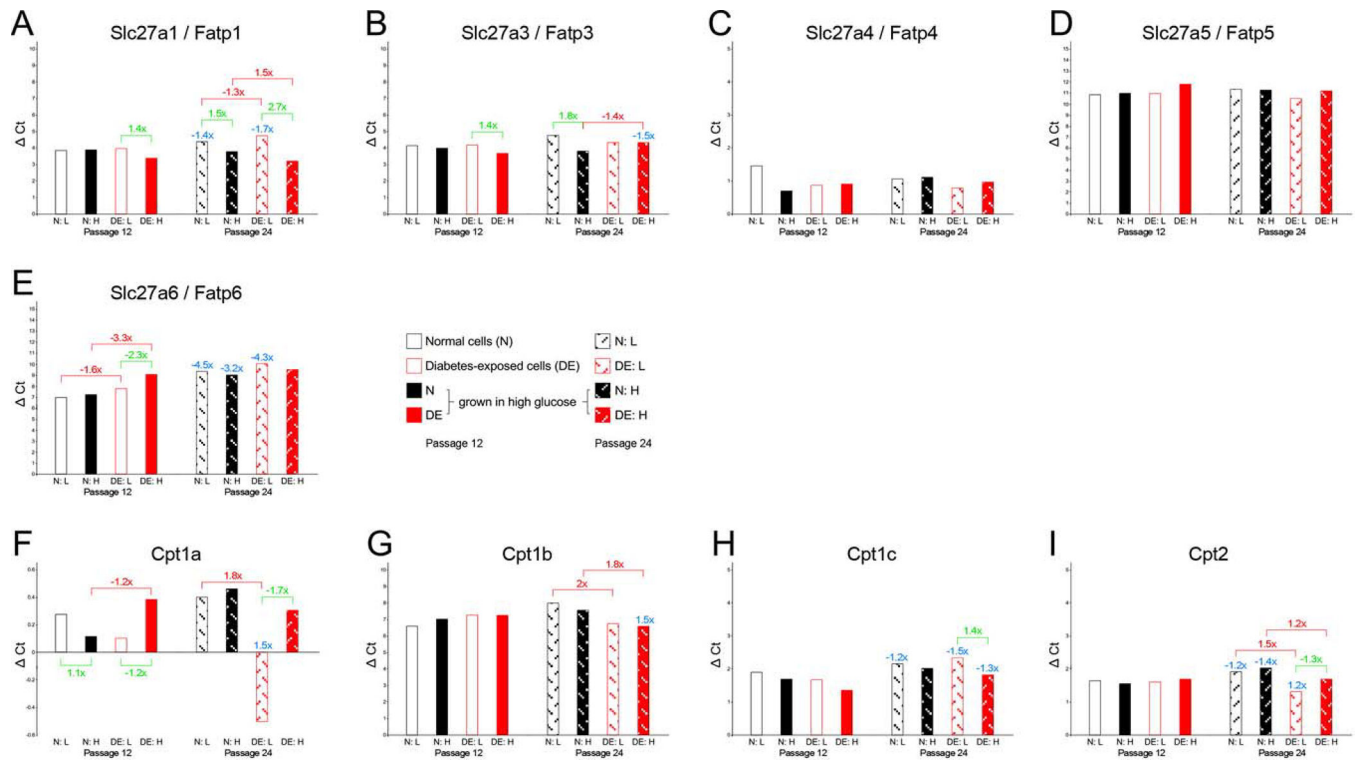


**Figure 7. Expression of nutrient transporters as assayed by quantitative real-time PCR: fatty acid transporters**

Expression levels are expressed in Cycle threshold (Ct) values, relative to the references gene averages (see Methods for details), with each sample measured in triplicate on the same assay plate. Standard deviations for the technical replicates are not depicted because they were negligible. Higher bars (larger Ct values) correspond to lower expression levels, smaller Ct values (lower bars) reflect higher expression levels. Fold-changes are given for significant differences in expression level when compared for the same condition between passage 12 and passage 24 (blue numbers), for comparisons of the same cell line in different maintenance media conditions (green numbers), and for differences between normal and diabetes-exposed cells (red numbers). Note that Y-axes have different scales for different genes.

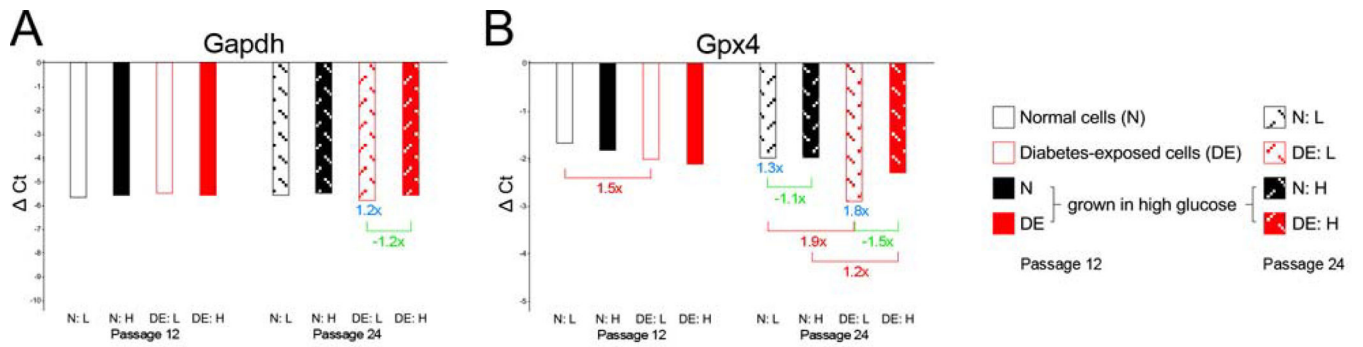


**Figure 8. Expression of genes related to oxidative stress.**

Because Gapdh and Gpx4 were expressed at higher levels than the average of the reference genes, the  $\Delta Ct$  values calculated are negative. Larger negative  $\Delta Ct$  values correspond to higher expression levels, smaller negative  $\Delta Ct$  values reflect lower expression levels. Otherwise, results are depicted analogous to Figures 6 and 7.

**Table 1:**

Sequences and characteristics of primers used for quantitative real-time PCR

Gene symbol	ENSEMBL Gene ID	Forward		Reverse		Exon-exon boundary		AE
		primer	primer	Position	primer	Position	boundary	
Cd36	ENSMUSG0000002944	GAACCTATTGAAGGCTTACATCCAA	1063-1087	TCCAGTTATGGGTTCACATCTAA	1134-1111	yes	1.85	
Cpt1a	ENSMUSG00000024900	CCAAACCCACCAGGCTACAG	1625-1644	AACCTGGCAGCTGTAGGGATGT	1702-1681	yes	1.90	
Cpt1b	ENSMUSG00000078937	CCCGAGCAGTGCCTGGGAGC	1652-1671	GAAATGAGCCAGCTGTAGGG	1822-1803	yes	1.81	
Cpt1c	ENSMUSG00000007783	GACAACAAGGAGACAGACCAACAT	2116-2139	CCCTTCAGTAGAGCCTGGTGCTT	2191-2170	yes	1.88	
Cpt2	ENSMUSG00000028607	TGGGCCAGGGCTTTTGAC	1787-1803	ATGTTGTGGTTTATCCGCTGGTA	1901-1879	yes	1.89	
Crat	ENSMUSG00000026853	ATGAGCATGCAGCTGCAGAA	1258-1277	GCGTAAGAGGTGTCCATGAAGA	1867-1846	yes	1.90	
Gapdh	ENSMUSG00000057666	CCAGAACATCATCCCTGCATC	649-669	GGTAGGAACAGGGAAGGCC	751-733	no	1.93	
Gpx4	ENSMUSG000000075706	AGGCAGGAGCCAGGAAGTAATC	499-520	CACAGATCTTGTCTGTACATGTCAAA	583-559	yes	1.96	
Pak1ip1	ENSMUSG00000038683	GCCCTGACCAACC TAAGACAAT	12661287	GCTTGTCTGCACCACTTACATCA	1370-1348	yes	1.92	
Pole4	<a href="#">ENSMUSG00000030042</a>	CGGGACAGGAAGCCATCTT	269-287	AGCAGTAGGCATCTTTTGGGATA	346-324	yes	1.90	
Slc27a1	ENSMUSG000000031808	AGATTGCCACAGCGTTTTTC	1629-1648	CATCACTAGCACAGTCACCTGAGA	1693-1671	yes	1.90	
Slc27a2	ENSMUSG000000273559	CGTCACGGTCAATCAGTACATTG	1663-1685	TTGGTTTCTGCGGTGTGTG	1727-1708	yes	1.85	
Slc27a3	ENSMUSG00000027932	CCCGACCTCGGTTCTCA	1939-1956	CATCTAAACCTTCTGCTGTTTGAA	2012-1989	yes	1.88	
Slc27a4	ENSMUSG00000059316	CTTTGTGTACCCTATCCGTTTGG	1566-1588	GGCCTGGCTGACCTGGTT	1669-1652	yes	1.90	
Slc27a5	ENSMUSG00000030382	CCTGAGCAACCAGAAGACAAGA	1262-1283	CATTTGCCCGAAGTCCATTG	1328-1309	yes	1.90	
Slc27a6	ENSMUSG00000024600	CGTGACTGTGTTTTCAGTACATTGG	1119-1142	CCTTCTCTGAGGCTGTTTC	1184-1163	yes	1.87	
Slc2a1	ENSMUSG000000028645	GGGCATGTGCTTCCAGTATGT	1498-1518	ACGAGGAGCACCGTGAAGAT	1569-1550	yes	1.90	
Slc2a2	ENSMUSG00000027690	CCGGATGATTGGCATGT	1109-1126	GTCATGCTCACGTAACCTCATCCA	1202-1180	yes	1.89	
Slc2a3	ENSMUSG00000003153	TTGCTCCGTTTTTCATGACGAT	1161-1181	GGGCCAGGTCCTCAATCTCAA	1277-1259	yes	1.89	
Slc2a4	ENSMUSG000000018566	CCGGCAGCCTCTGTATCAT	1020-1037	CGACTCGAAGATGCTGGTTGA	1116-1096	yes	1.90	
Slc2a5	ENSMUSG00000028976	GGCGCTGCAGAACACCAT	1800-1817	AAGCGGTGCTTATGACGTAGAC	1877-1855	yes	1.90	
Slc2a6	ENSMUSG00000036067	CAGCCTTCGTCCTCACTAATCTT	1394-1418	GGAGATGGCCGAGAGAAGA	1480-1462	yes	1.88	
Slc2a7	ENSMUSG000000062064	AGCCCCGCTACACTCTGA	700-718	GCAGCCTCTTAGAGCTTGTCT	766-745	yes	1.90	
Slc2a8	ENSMUSG000000026791	TCGGTCACTGTGGCATAATC	955-975	CCCTGTCTGTCCATGATGA	1023-1004	no	1.87	
Slc2a9	ENSMUSG00000005107	GGCCTGAACACTGAGAATGAC	2475-2496	TACATCCAGGACAGACATCATCAA	2563-2540	no	1.89	
Slc2a10	ENSMUSG000000027661	AAGCAGGTTCCCTCTAAACTTTGG	1788-1811	CATCCAGGCGATGGTACTGA	1852-1833	yes	1.87	
Slc2a12	ENSMUSG000000037490	CAAAGGGCAACTATGTGAAAAACA	1897-1920	TTACACTCTGGGAGCTGCTCTTG	2008-1986	yes	1.87	

Author Manuscript

Author Manuscript

Author Manuscript

Author Manuscript

Gene symbol	ENSEMBL Gene ID	Forward primer	Reverse primer	Position	Position	AE
Sic2a13	ENSMUSG00000036298	GACTCCTTCGGATCAAAAATACCA	TGTAGCAGAAAACCCACAGTCTGGAT	1412-1434	1497-1474	yes 1.83